C. R. Palevol 11 (2012) 419–433

Contents lists available at SciVerse ScienceDirect

Comptes Rendus Palevol

www.sciencedirect.com

General palaeontology, systematics and evolution (Vertebrate palaeontology)

Palaeobiology of Triassic procolophonids, inferred from bone microstructure

Paléobiologie des procolophonidés triasiques déduite de leur microstructure osseuse

Jennifer Botha-Brink[a,*], Roger Malcolm Harris Smith[b]

[a] *Karoo Palaeontology, National Museum, Box 266, Department of Zoology and Entomology, University of the Free State, 9300 Bloemfontein, South Africa*
[b] *Karoo Palaeontology, Iziko South African Museum, Box 61, Department of Geology, University of Cape Town, 8000 Cape Town, South Africa*

ARTICLE INFO

Article history:
Received 20 September 2011
Accepted after revision 5 March 2012
Available online 2 July 2012

Presented by Philippe Taquet

Keywords:
Procolophonidae
Procolophonid
Bone histology
End-Permian extinction
South Africa
Karoo Basin

ABSTRACT

Procolophonoidea represent the most successful radiation of Parareptilia that lived during the Permo-Triassic. They are one of the few vertebrate groups that survived the end-Permian extinction and are thus important for studying the recovery of the post-extinction terrestrial ecosystem. Here, we investigate the palaeobiology of three Triassic procolophonid parareptiles, namely *Sauropareion anoplus*, *Procolophon trigoniceps* and *Teratophon spinigenis*, from the Karoo Basin of South Africa, inferred from histological analyses of their limb bones. Results reveal that all three taxa exhibit parallel-fibered bone tissue. Growth rings are absent in the Early Triassic *Sauropareion* and *Procolophon* whereas annuli are present in the Middle Triassic *Teratophon*, even during early ontogeny, suggesting a difference in life histories. Morphology and bone histology imply fossorial lifestyles for all three taxa, suggesting that burrowing may have played an important role in their survival during the harsh post-extinction Triassic environment.

Mots clés :
Procolophonidae
Procolophonide
Histologie osseuse
Extinction permo-triasique
Afrique du Sud
Bassin du Karoo

RÉSUMÉ

Les Procolophonidea représentent la plus grande radiation évolutive des Parareptiles permo-triasiques. Ils composent l'un des quelques groupes de vertébrés ayant survécu à l'extinction de la fin du Permien et sont donc importants pour étudier la récupération de l'écosystème terrestre après la crise biologique. Dans cet article, nous examinons la paléobiologie de trois parareptiles procolophonides triasiques, plus particulièrement *Sauropareion amoplus*, *Procolophon trigoniceps* et *Teratophon spinigenis* du bassin du Karoo en Afrique du Sud, déduite de l'analyse histologique des os de leurs membres. Les résultats révèlent que les trois taxa montrent un tissu osseux à fibres parallèles. Les anneaux de croissance sont absents chez *Sauropareion* et *Procolophon*, du Trias inférieur, tandis qu'ils sont présents chez *Teratophon*, du Trias moyen, même dans les stades précoces de l'ontogenèse, ce qui indiquerait une différence dans leurs histoires de vie. La morphologie et l'histologie osseuse impliquent un style de vie fouisseur pour les trois taxons, ce qui suggère que le fouissage peut avoir joué un rôle important dans leur survie dans les conditions environnementales sévères après la crise permo-triasique.

* Corresponding author.
E-mail addresses: jbotha@nasmus.co.za (J. Botha-Brink), rsmith@iziko.org.za (R.M.H. Smith).

1631-0683/$ – see front matter
doi:10.1016/j.crpv.2012.03.002

1. Introduction

Parareptiles were a diverse group of reptiles with a global distribution whose first appearance dates back to the Earliest Permian, some 297 Ma (million years ago) (Tsuji and Müller, 2009). As the sister group of Eureptilia, they are one of the few major amniote clades that survived the end-Permian extinction (Ruta et al., 2011). This event occurred 252.6 Ma (Mundil et al., 2004) and is considered to be the greatest mass extinction in Earth's history. Although parareptiles such as the aquatic mesosaurs, lizard-like millerettids and large herbivorous pareiasaurs went extinct during the Early to Late Permian, the Procolophonoidea were the only parareptiles to survive the end-Permian extinction (Botha et al., 2007; Ruta et al., 2011).

Two families are usually recognized in the Procolophonoidea, namely Owenettidae and Procolophonidae (Modesto and Damiani, 2007). The latter group (Fig. 1) comprises small, lizard-like parareptiles, all of which (apart from the Russian procolophonid *Suchonosaurus* Säilä, 2009) lived during the Early and Middle Triassic (Cisneros, 2008). Although the taxonomy of Procolophonidae has received more attention in recent years, due to the discovery of several new species (e.g., *Coletta seca*, Gow, 2000; *Sauropareion anoplus*, Modesto and Damiani, 2007; *Phonodus dutoitorum*, Modesto et al., 2010), the palaeobiology of this group remains enigmatic.

Studying the microstructure of bone provides information about the biology of an animal (Enlow and Brown, 1957, 1958). This technique can be used to assess growth rates, individual longevity and changes during ontogeny, information that cannot necessarily be gained using more traditional methods such as morphometrics and comparative analysis. The Triassic procolophonid parareptiles are a particularly interesting group as they were not severely affected by the environmental changes that resulted in the end-Permian extinction (Modesto and Damiani, 2003; Modesto et al., 2001). Consequently, understanding their biology may provide clues as to why this group was left relatively unscathed by the extinction event.

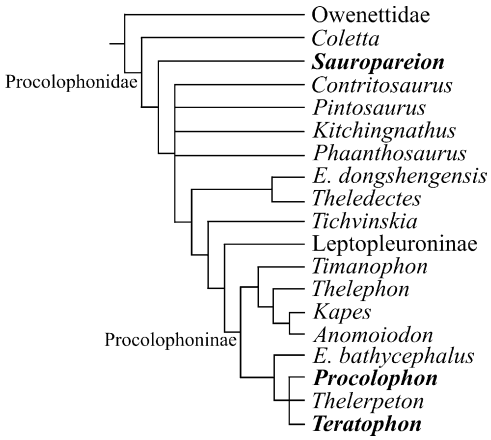

Fig. 1. Phylogeny of Procolophonidae. Taxa examined in this study are in bold. Phylogeny taken from Cisneros (2008) and Tsuji and Müller (2009). Abbreviation: E: *Eumetabolodon*.

Fig. 1. Phylogénie des Procolophonidae. Les taxa examiné dans cette étude sont en gras. La phylogénie est proposée d'après Cisneros (2008) et Tsuji et Müller (2009). Abréviation : E : *Eumetabolodon.*

2. Material and methods

Three species of procolophonid parareptiles were examined, namely *Sauropareion anoplus* and *Procolophon trigoniceps* from the Lower Triassic *Lystrosaurus* Assemblage Zone, and *Teratophon spinigenis* from the Middle Triassic *Cynognathus* Assemblage Zone, all from the Karoo Basin of South Africa (Fig. 1; Table 1). We spent two field seasons collecting postcranial material of *P. trigoniceps* for the purpose of thin sectioning. As this species is by far (by orders of magnitude) the most abundant Triassic procolophonid in Karoo strata, we were able to collect 18 limb bones for bone histological analysis. This study material includes several limb bones from single individuals as well as homologous elements from numerous specimens, allowing us to consider inter-elemental and inter-individual variation. In addition, this relatively large sample size includes limb bones of varying ontogenetic status facilitating an assessment of histological changes through ontogeny (Table 1). In contrast, only five specimens of *S. anoplus* and 11 specimens of *T. spinigenis* have been positively identified. Thus, only a single individual of *S. anoplus* and two individuals of *T. spinigenis* were available for thin sectioning (Table 1). All specimens were positively identified using associated skull material, apart from SAM-PK-7711, NMQR 3565 and NMQR 3555. The latter two specimens are postcranial material collected from the Katberg Formation (middle *Lystrosaurus* Assemblage Zone). They are identified as *P. trigoniceps* and distinguished from *S. anoplus* by the similarity of the interclavicles to known *Procolophon* interclavicles and the particularly robust humerus with a prominent entepicondylar foramen. Specimen SAM-PK-7711 is a large, almost complete procolophonid skeleton with no skull. deBraga (2003) included this specimen in his description of the postcrania of *P. trigoniceps*. However, it was collected from the Aliwal North Quarry in the Middle Triassic *Cynognathus* Assemblage Zone, which is above the known stratigraphic range of *Procolophon* (Botha and Smith, 2006). As the specimen is large and robust, Cisneros (2008) tentatively assigned the specimen to *T. spinigenis*, the largest procolophonid known from the *Cynognathus* Assemblage Zone. However, as Modesto and Damiani (2003) noted, all positively identified procolophonid taxa from the *Cynognathus* Assemblage Zone are based solely on skull material. Thus, Cisneros (2008) could not use any characters to unequivocally identify specimen SAM-PK-7711 as *T. spinigenis*. Consequently, the assignment of SAM-PK-7711 to *T. spinigenis* must remain tentative until more positively identifiable postcranial material of *T. spinigenis* is recovered. Despite the problematic specific identification of SAM-PK-7711, the specimen represents the largest, best preserved procolophonid known from the Middle Triassic *Cynognathus* Assemblage Zone, and can thus, provide important information regarding the biology of procolophonids from this biozone.

Table 1
Specimens thin sectioned in this study. The percentage maximum size was estimated using the largest known specimens for each genus. *Sauropareion anoplus* and *Procolophon trigoniceps* are from the Lower Triassic *Lystrosaurus* Assemblage Zone and *Teratophon spinigenis* is from the Middle Triassic *Cynognathus* Assemblage Zone, all from the South African Karoo Basin. "*k*" refers to the ratio between the internal and external diameter of the bone (Currey and Alexander, 1985) and "*C*" refers to the global bone compactness (Girondot and Laurin, 2003), i.e. the ratio between mineralised bone surface and section (including the medullary area). Measurements are in millimeters.

Tableau 1
Spécimens étudiés en lame mince. La taille maximum en pourcentage a été estimée en utilisant les plus grands spécimens connus pour chaque genre. *Sauropareion anoplus* et *Procolophon trigoniceps* proviennent de la zone d'assemblage du Trias inférieur à *Lystrosaurus* et *Teratophon spinigenis* est issu de la zone d'assemblage du Trias moyen à *Cynognathus*, tous du bassin du Karoo, en Afrique du Sud. « *k* » correspond au rapport entre diamètre interne et externe de l'os (Currey et Alexander, 1985) et « *C* » à la compacité globale de l'os (3), i.e. le rapport entre la surface et la section de l'os minéralisé (incluant la zone médullaire). Les mesures sont en millimètres. Comm. : Commonage ; Mbg : Middleburg District ; Rville : Rouxville District.

Genus	Accession number	Locality	Skull length	Total length	Midshaft width	Proximal width	Distal width	% size	% cortical porosity	*k*	*C*
S. anoplus											
Radius	NMQR 3602	Vangfontein, Mbg	33	20.1	2.7	3.4	9.8	–	3.4	0.56	–
P. trigoniceps											
Humerus	NMQR 3608	Vangfontein, Mbg	31.4	–	2.9	–	–	40	–	–	–
Tibia	NMQR 3588	Vangfontein, Mbg	36.2	16.1	2.6	7.7	4.1	46	3.4	0.69	0.479
Humerus	NMQR 3944a	Bloemfontein	39	25.6	3.1	11.2	–	51	–	0.39	–
Femur	NMQR 3944b	Bloemfontein	39	29.4	4.3	10.2	8.8	51	7.5	0.6	0.576
Tibia	NMQR 3944c	Bloemfontein	39	19.3	3.2	7.6	5.2	51	–	0.48	–
Radius	NMQR 3572	Vangfontein, Mbg	40.7	–	3.4	–	–	52	–	–	–
Humerus	NMQR 3565a	Vangfontein, Mbg	–	26.7	3.1	11.5	12	53	4.4	0.42	0.692
Radius	NMQR 3565b	Vangfontein, Mbg	–	19.5	2.6	–	5.1	53	–	0.53	0.653
Tibia	NMQR 3591	Unknown	–	21.2	3.9	2	3.6	54	2.7	0.43	0.791
Humerus	NMQR 3555a	Vangfontein, Mbg	–	28.3	3.9	11.6	16	57	–	0.38	–
Femur	NMQR 3555b	Vangfontein, Mbg	–	30	4.4	–	8.7	57	10.6	0.56	0.602
Humerus	NMQR 3945	Vangfontein, Mbg	–	–	4.3	–	–	62	3.8	0.66	0.501
Humerus	SAM-PK-K10727a	Glenridge, Albert	56.7	31.3	4.9	8.8	16.3	73	–	–	–
Radius	SAM-PK-K10727b	Glenridge, Albert	56.7	30	3	6	4.3	73	6	0.59	0.639
Ulna	SAM-PK-K10727c	Glenridge, Albert	56.7	23.2	4.1	7.7	6.6	73	4.4	0.44	0.763
Humerus	NMQR 3622a	Vangfontein, Mbg	60	38	5.3	–	22.4	77	4.2	0.62	0.632
Radius	NMQR 3622b	Vangfontein, Mbg	60	27.3	3.2	7.1	6.7	77	4.4	0.62	0.666
Radius	NMQR3676	Temple Farm, Mbg	64	–	3.5	8.4	–	82	6.7	–	–
T. spinigenis											
Radius	SAM-PK-10183	Lemoenfontein, Rville	~40	16.8	2.5	3.2	–	55	2.5	0.32	0.896
Humerus	SAM-PK-7711a	Aliwal North Comm.	–	48.4	6.5	22.2	24.8	100	6.3	0.31	0.834
Tibia	SAM-PK-7711b	Aliwal North Comm.	–	35.4	5.5	13.8	–	100	5.4	0.33	0.833

Comm.: Commonage; Mbg: Middelburg District; Rville: Rouxville District.

Limb bones were selected for thin sectioning because they contain the least secondary remodelling in the mid-shaft regions and consequently exhibit the most complete growth record of the animal (Francillon-Vieillot et al., 1990; Horner et al., 1999). The bones were measured and photographed before sectioning, and ontogenetic age was estimated for each element from dimensions of the largest known specimens of *P. trigoniceps* and *T. spinigenis*. The largest known specimen of *S. anoplus* is the holotype SAM-PK-11192 and was still actively growing at the time of death (determined from the open axial neurocentral suture and incomplete ossification of the distal end of the associated humerus; Modesto and Damiani, 2007; Modesto et al., 2001). Thus, all known specimens of *Sauropareion* are considered to be juveniles. The thin sectioning was conducted at the National Museum, Bloemfontein, following procedures outlined by Chinsamy and Raath (1992) with some minor modifications. The bone microstructure was viewed and photographed using a Nikon Eclipse 50i Polarizing microscope and DS-Fi1 digital camera. Bone histology terminology follows that of Francillon-Vieillot et al. (1990) and Reid (1996).

As the organization and density of the vascular canals in cortical bone is closely related to bone apposition rate (e.g., Amprino, 1947; de Margerie et al., 2002), the area occupied by these canals in a given bone section provides a quantitative method for comparing vascular density between different taxa. This quantification reflects the maximum possible vascularization for each element, as the channels would have contained lymph and nerves as well as blood vessels (Starck and Chinsamy, 2002). The total canal area was quantified using the image analysis program NIH ImageJ, which was then divided by the total cortical area and expressed as a percentage. The higher the vascular density, the more porous the bone.

The structure of the bone wall of an animal varies according to factors such as lifestyle, ontogeny and biomechanical demands (e.g., Canoville and Laurin, 2010; Cubo et al., 2005; Germain and Laurin, 2005; Kriloff et al., 2008; Wall, 1983). For example, a particularly thick cortex may reflect an aquatic (e.g., de Buffrénil et al., 1990; Hua and de Buffrénil, 1996; Wall, 1983) or fossorial (burrowing) lifestyle (e.g. Biknevicius, 1993; Botha, 2003; Lagaria and Youlatos, 2006). In this study, we report the thickness of the bone wall by calculating the diaphyseal cortical thickness or "*k*" (Currey and Alexander, 1985), which is the ratio between the inner diameter and outer diameter of the bone. Cortical thickness is thinnest when *k* tends towards 1 (i.e. no bone walls), and thickest when *k* tends towards 0 (i.e. solid bone) (Currey and Alexander, 1985).

Bone compactness (defined as "the ratio between the surface occupied by bone tissues and the total bone surface", Germain and Laurin, 2005:337) was also calculated using the computer program Bone Profiler for Windows (Girondot and Laurin, 2003). Among other things, this software calculates the ratio between the mineralized tissue surface and the total cross-sectional surface and reveals the global compactness of the bone (Canoville and Laurin, 2010; Germain and Laurin, 2005; Girondot and Laurin, 2003; Laurin et al., 2004). Compactness is lower towards 0 and higher towards 1.

3. Results

3.1. Lystrosaurus Assemblage Zone Procolophonids

3.1.1. Sauropareion anoplus

All known *Sauropareion* specimens, including NMQR 3602, are similar in size and considered to be juveniles. A transverse section through the midshaft of the humerus of NMQR 3602 reveals poorly preserved bone tissue, where only a few regions are preserved well enough for analysis. The bone contains a moderately thick bone wall ($k = 0.56$) and a large, clear medullary cavity that is devoid of bony trabeculae (Fig. 2A). The bone tissue consists of uninterrupted parallel-fibered bone (defined as a bone matrix consisting mostly of mutually parallel collagenous fibers, sometimes flattened osteocyte lacunae and simple primary vascular canals and/or primary osteons, Francillon-Vieillot et al., 1990; Reid, 1996), as seen by the mass birefringence (Fig. 2B), with flattened or oval osteocyte lacunae. The osteocyte lacunae are organized in parallel rows. Sparse, simple, longitudinally or radially-oriented vascular canals (Fig. 2C, D) are distributed randomly throughout the cortex (average diameter 24 μm). Although the vascularization for the whole cortex could not be quantified, one field of view revealed that the canals occupied 3.4% of the cortical area.

3.1.2. Procolophon trigoniceps

The 18 *Procolophon* limb bones were assigned size classes based on the length of their associated skulls in proportion to the maximum known skull length, which is 78 mm (BP/1/4248) and considered to be an adult (Cisneros, personal communication, 2011). The size classes comprise sub-adult (31–59% maximum size; size class II), late sub-adult (60–79% maximum size; size class III) and adult (80–100% maximum size; size class IV) (Botha-Brink and Angielczyk, 2010). None of the specimens in this study fell into the juvenile age class (0–30% maximum size; size class I).

3.1.3. Size class II

Specimens NMQR 3608 and NMQR 3588 are the smallest individuals examined in this study and are estimated to be 40% and 46% of the maximum known size for *Procolophon*, respectively. The humerus from NMQR 3608 and the tibia from NMQR 3588 both contain relatively thin cortices and large free medullary cavities (although cortical thickness could not be quantified in NMQR 3608 due to incomplete preservation). The osteocyte lacunae are preserved only in patches. They are abundant, globular and randomly distributed throughout the cortex in a parallel-fibered bone matrix. Vascularization is poor (NMQR 3588 = 3.4% cortical porosity) and consists of longitudinally-oriented simple vascular canals (average diameter 22 μm). Growth rings in the form of annuli (narrow translucent zones consisting of parallel-fibered bone or lamellar bone with sparse, flattened osteocyte lacunae and corresponding to periods of slow growth, Francillon-Vieillot et al., 1990) or Lines of Arrested Growth (LAG, cementing lines that correspond to temporary, but complete cessations in growth, Francillon-Vieillot et al., 1990) are absent. There is no evidence of any

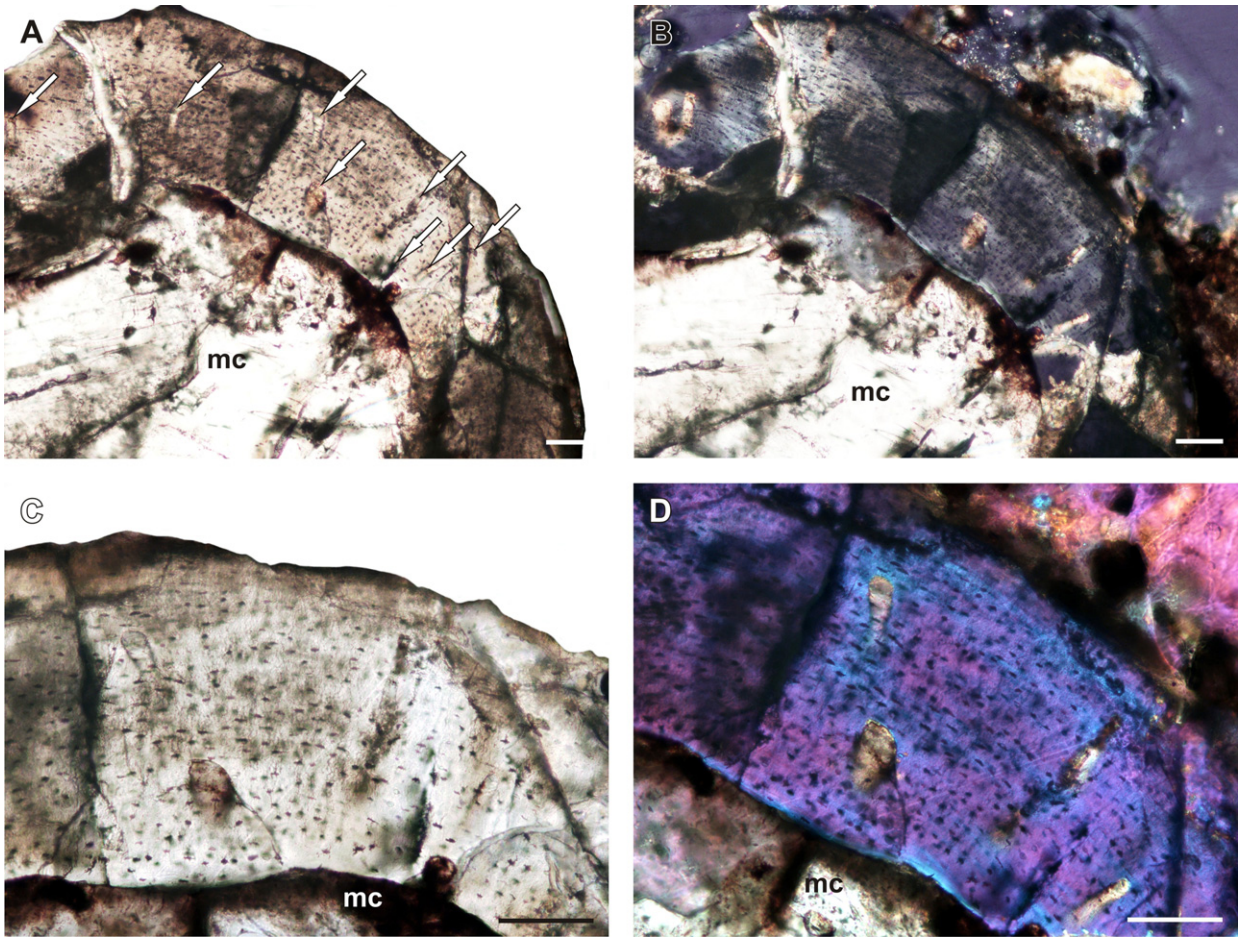

Fig. 2. Bone histology of *Sauropareion anoplus*, NMQR 3602. **A**. Transverse section of the humerus through the midshaft region showing a highly organized bone tissue with sparse vascular canals (arrows). **B**. Transverse section in polarized light showing parallel-fibered bone tissue. **C**. High magnification showing simple vascular canals. **D**. High magnification in polarized light with Lambda compensator, showing a parallel-fibered bone matrix. Abbreviation: mc: medullary cavity. Scale bars 100 μm.

Fig. 2. Histologie osseuse de *Sauropareion anoplus*, NMQR. **A**. Section transversale de l'humérus à travers la région axiale montrant un tissu osseux très bien organisé avec des canaux vasculaires épars (flèches). **B**. Section transversale en lumière polarisée montrant un tissu osseux à fibres parallèles. **C**. Fort grossissement montrant des canaux vasculaires simples. **D**. Fort grossissement en lumière polarisée avec compensateur Lambda, montrant une matrice osseuse à fibres parallèles. Abréviation : mc : cavité médullaire. Barre d'échelle, 100 μm.

secondary remodelling and the medullary margin lacks any circumferential endosteal lamellae.

Five specimens range from 51% to 57% maximum size. The cortices of all the limb bones are moderately thick and bone compactness values range from 0.576 to 0.791 (Table 1). The overall bone tissue consists of poorly vascularized (2.7% in tibia NMQR 3591) to relatively highly vascularized (6.7% in femur NMQR 3944b and 10.6% in femur NMQR 3555b) parallel-fibered bone (Fig. 3A–C). The osteocyte lacunae vary from flattened to globular in shape (Fig. 3D). They are highly abundant and randomly distributed in regions of the femora and humeri (Fig. 3E), but are also organized in parallel rows in some regions of the femora (Fig. 3C) and humeri and in most of the cortex in the radii, ulnae and tibiae. The vascular canals are mostly longitudinally-oriented simple canals (average diameter 25 μm), but form a reticular organization in the femora (average diameter 44 μm) and extend radially from the medullary cavity in the radii and tibiae. A few poorly-defined primary osteons are present in the humerus and femur of NMQR 3555, where they also become radially-oriented in the humerus. The primary osteons average 55 μm in diameter. Secondary osteons and growth rings were not observed in any of the limb bones. A thin layer of circumferential endosteal lamellae was observed in the perimedullary region of humerus NMQR 3944a (51% maximum size) and the humerus and femur of individual NMQR 3555 (57% maximum size). Sharpey's fibers (indicating regions of muscle insertions) were observed in the humeri, ulnae (Fig. 3F) and tibiae in the regions of the deltopectoral, ulnar and cnemial crests, respectively.

3.1.4. Size class III

Three specimens, namely NMQR 3945, SAM-PK-K10727 and NMQR 3622, are 62%, 73% and 77% of the maximum size respectively, and are thus classified as late sub-adults. The

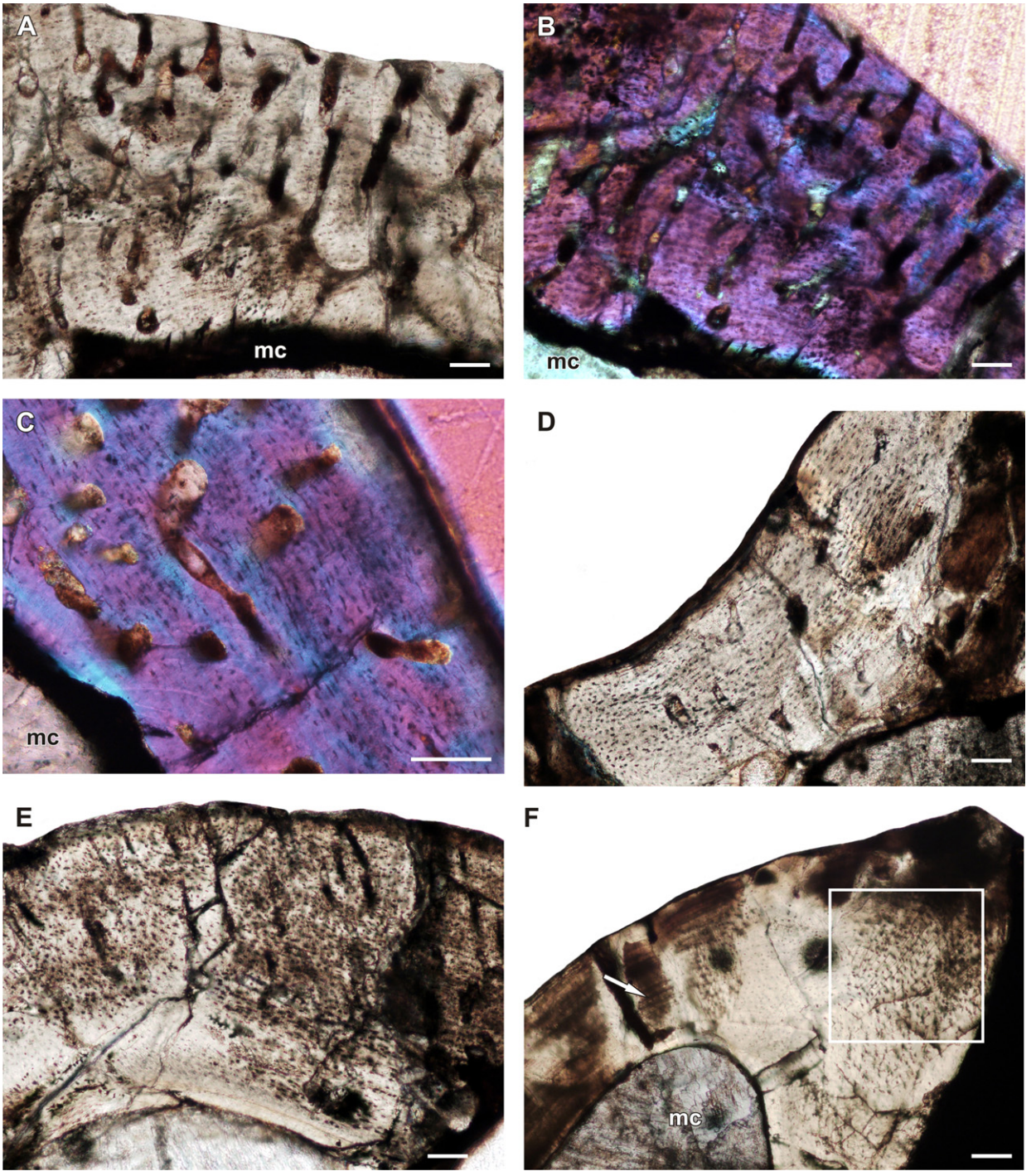

Fig. 3. Bone histology of *Procolophon trigoniceps*. **A.** Femur of NMQR 3944b showing numerous large vascular canals. **B.** Femur of NMQR 3944b in polarized light with Lambda compensator, showing parallel-fibered bone. **C.** Femur of NMQR 3555b in polarized light with Lambda compensator showing numerous large vascular canals and highly organized osteocyte lacunae in parallel-fibered bone. **D.** Humerus of NMQR 3565a showing a mixture of oval (left) and flattened (right) osteocyte lacunae. **E.** Humerus of NMQR 3944a showing highly abundant randomly distributed osteocyte lacunae. **F.** Tibia of NMQR 3944c showing parallel-fibered bone and Sharpey's fibers (box). Abbreviation: mc: medullary cavity. Scale bars 100 μm.

Fig. 3. Histologie osseuse de *Procolophon trigoniceps*. **A.** Fémur de NMQR 3944b montrant de nombreux grands canaux vasculaires. **B.** Fémur de NMQR 3944b en lumière polarisée avec compensateur Lambda, montrant que l'os est constitué, qu'il est constitué d'os à fibres parallèles. **C.** Fémur de NMQR 3555b en lumière polarisée avec compensateur lambda montrant de nombreux grands canaux vasculaires et des lacunes d'ostéocyte très bien organisées dans l'os à fibres parallèles. **D.** Humérus de NMQR 3565a montrant un mélange de lacunes d'ostéocyte ovales (à gauche) et aplaties (à droite). **E.** Humérus de NMQR 3944a montrant de très nombreuses lacunes ostéocytaire distribués au hasard. **F.** Tibia de NMQR 3944c montrant un os à fibres parallèles et des fibres de Sharpey (dans le carré blanc). Abréviation : mc : cavité médullaire. Barre d'échelle 100 μm.

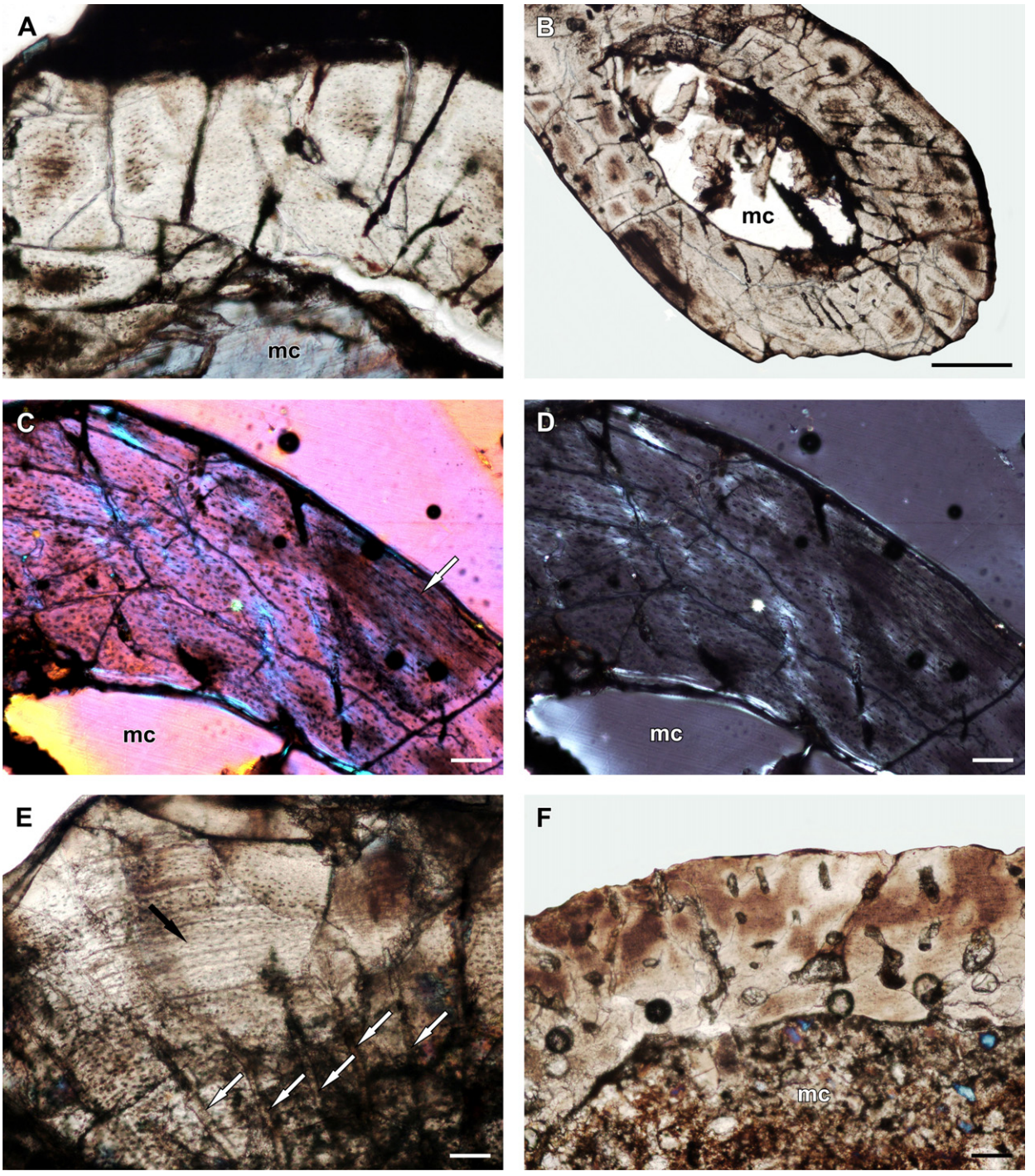

Fig. 4. Bone histology of *Procolophon trigoniceps*. **A.** Radius of SAM-PK-K10727b showing parallel-fibered bone with simple radial canals. **B.** Ulna of SAM-PK-K10727c showing radial simple canals in a poorly vascularized bone tissue. **C.** Ulna of SAM-PK-K10727c in polarized light with Lambda compensator showing parallel-fibered bone and an increase in osteocyte lacunae organization at the bone periphery (arrow). **D.** Ulna of SAM-PK-K10727c in polarized light showing parallel-fibered bone. **E.** Humerus of NMQR 3622a showing numerous radially-oriented vascular canals (white arrows) in the inner cortex and increased organization in the osteocyte lacunae with a dramatic decrease in vascularization (black arrow) in the outer cortex. **F.** Radius of NMQR 3676 showing relatively large vascular canals in parallel-fibered bone tissue. Abbreviation: mc: medullary cavity. Scale bars 100 μm, apart from (**B**) 500 μm.

cortices of the bones in all specimens are moderately thick ($k = 0.44$ to 0.66; Table 1) and the medullary cavities are large and free of trabecular infilling. The bone tissue of all elements contains abundant, globular or flattened osteocyte lacunae in a parallel-fibered bone matrix (Fig. 4A–F). The vascular canals vary between longitudinally-oriented simple canals with short anastomoses (average diameter 17.6 μm) and radiating vascular canals (Fig. 4A–C, E). There is a clear decrease in the number of vascular canals towards the periphery of humerus NMQR 3622 (Fig. 4E). This region also shows a decrease in the number of osteocyte lacunae. Growth rings are absent in all elements and secondary remodelling was only observed in the ulna in the form of a few large resorption cavities in the perimedullary region. Sharpey's fibers were also observed in this element.

3.1.5. Size class IV

One radius in this study (NMQR 3676) was classified as 82% maximum size (Table 1). It is poorly preserved and incomplete, and only the proximal region could be thin sectioned. A relatively thin cortex reveals a poorly organized parallel-fibered bone tissue with numerous longitudinally and radially-oriented simple canals (cortical porosity 6.7%; average diameter 24 μm) (Fig. 4F). The medullary cavity is completely free of trabeculae and growth rings are absent.

3.1.6. Inter-elemental histovariation in Procolophon

Differences in vascular orientation and density were observed between the various *Procolophon* limb bones. The humeri and femora are more vascularized than the epipodial elements (radius, ulna, tibia). The femora contain a mixture of relatively large longitudinally and radially-oriented vascular canals as well as those in a reticular organization. In contrast the humeri, radii, the ulna and larger tibia contain primarily radially-oriented vascular canals (Fig. 5). The simple vascular canals observed in the radii, ulna and tibia are relatively smaller than those in the humeri and femora. Primary osteons, which are closely linked with rapid bone deposition rates (de Margerie et al., 2002), were observed in the propodial elements, but are absent from the epipodials. As vascularization is closely related to growth rates (Amprino, 1947; de Margerie et al., 2002), the presence of primary osteons as well as the overall higher vascular density implies a relatively higher rate of bone deposition in the propodials than in the epipodials.

3.2. Cynognathus Assemblage Zone Procolophonids

SAM-PK-K10183 is a radius taken from a positively identified (associated with skull) specimen of *T. spinigenis*. The bone is approximately 55% of the maximum known size for this taxon. The cortex is notably thick ($k = 0.32$) and compact ($C = 0.896$), and the medullary cavity only contains one or two trabeculae. The bone tissue consists of a well-defined parallel-fibered bone matrix (Fig. 6A, B). The osteocyte lacunae are flattened and highly abundant. Vascularization is poor (2.5%) and consists of some longitudinally-oriented simple canals (average diameter 17 μm), but mostly radially-oriented canals that reach the periphery, giving the bone an uneven subperiosteal surface. A few primary and secondary osteons were observed in the inner cortex, and several large resorption cavities are present in the perimedullary region. A thin layer of circumferential endosteal lamellar bone was also observed. A few faint lines consisting of an increased abundance of osteocyte lacunae traverse the mid-cortex, suggesting some type of variation in growth rate. They do not appear to be annuli or LAG as the localized increased number of osteocytes suggests a temporary increase in growth rate. Prominent and abundant Sharpey's fibers were observed throughout the cortex (Fig. 6B).

The humerus and tibia of SAM-PK-7711, which have been tentatively assigned to *T. spinigenis*, revealed thick cortices (Table 1) surrounding mostly free medullary cavities. Some bony trabeculae traversed a portion of the medullary cavity in the tibial midshaft. The bone compactness values in the humerus and tibia are 0.834 and 0.833 respectively. Both humeral and tibial inner cortices (Fig. 6C–F) contain parallel-fibered bone tissue with relatively highly vascularized tissues with simple vascular canals (average diameter 36.3 μm in the humerus and 23.7 μm in the tibia), a few poorly developed primary osteons (average diameter 99 μm) and in the tibia, several small secondary osteons as well. Short anastomoses result in a reticular organization in the inner and mid-cortex of the humerus (Fig. 6C), whereas the tibia contains predominantly radially-oriented vascular canals. The inner bone tissue is interrupted by widely spaced annuli, but the annuli increase in number and become very closely spaced in the outer cortex in both elements (Fig. 6C, F). The vascular canals also decrease in size towards the periphery (average diameter 13 μm). Eight annuli were counted in the humerus, whereas only three annuli could be distinguished in the tibia prior to the onset of multiple, closely spaced annuli. Enlarged erosion cavities are present in the endosteal margins of both elements, but are more numerous in the tibia. Thin layers of inner circumferential lamellae surround the medullary cavities of both elements.

3.3. Inter-elemental histovariation in Cynognathus Assemblage Zone Procolophonids

The humerus of SAM-PK-7711 contains the highest vascularization amongst the *Cynognathus* Assemblage Zone elements. However, both the humerus and tibia of SAM-PK-7711 are notably more vascularized than the radius of

Fig. 4. Histologie osseuse de *Procolophon trigoniceps*. **A**. Radius de SAM-PK-K 10727b montrant un os à fibres parallèles avec de simples canaux radiaux. **B**. Ulna de SAM-PK-K 10727c montrant de simples canaux radiaux dans un tissu osseux faiblement vascularisé. **C**. Ulna de SAM-PK-K 10727c en lumière polarisée avec un compensateur lambda montrant un os à fibres parallèles et un accroissement dans l'organisation des lacunes d'ostéocyte à la périphérie de l'os (flèche). **D**. Ulna de SAM-PK-K 10727c en lumière polarisée montrant un os à fibres parallèles. **E**. Humérus de NMQR 3622a montrant de nombreux canaux vasculaires orientés radicalement (flèches blanches) dans le cortex interne et augmentation de l'organisation dans les lacunes d'ostéocyte avec diminution très importante de la vascularisation dans le cortex externe. **F**. Radius de NMQR 3676 montrant des canaux vasculaires relativement grands dans un tissu osseux à fibres parallèles. Abréviation : mc : cavité médullaire. Barres d'échelle 100 μm, sauf pour **(B)** 500 μm.

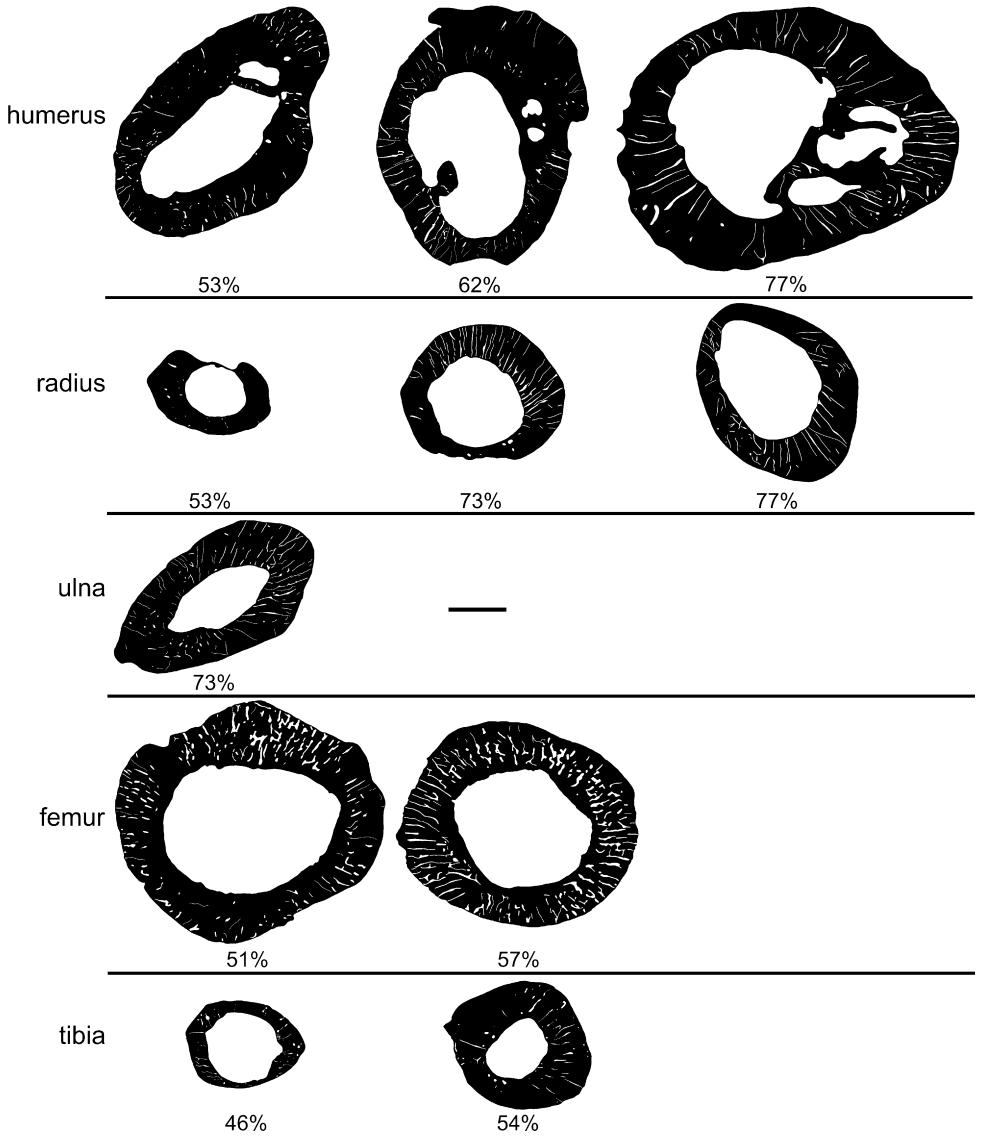

Fig. 5. Diaphyseal cross-sections of *Procolophon trigoniceps* limb bones from ontogenetically youngest (left) to ontogenetically oldest (right). Note the radiating vascular canals in the ulna and larger humeri and radii, as well as the high reticular vascularization in the femora. Percentages indicate percentage maximum size. Scale bar 1 mm.

Fig. 5. Coupes transversales diaphysaires dans des os de membre de *Procolophon trigoniceps* du plus jeune (à gauche) au plus vieux (à droite) ontogénétiquement parlant. À noter les canaux vasculaires rayonnants dans l'ulna et dans les grands humérus et radius, ainsi que la vascularisation hautement réticulée dans les fémurs. Les pourcentages sont ceux de la taille maximum. Barre d'échelle 1 mm.

SAM-PK-K10183 (Fig. 7). The vascular orientation also differs, where a reticular organization was observed in the inner and mid-cortex of the humerus, the canals radiate out from the medullary cavity in the tibia, and they are mostly longitudinally-oriented in the radius. The lower vascularization in the radius implies a slower overall growth rate for this element, compared to the humerus and tibia.

4. Discussion

4.1. Triassic procolophonid palaeobiology

The sparse simple vascular canals, absence of primary osteons and presence of highly organized osteocyte lacunae in the bone tissues of *S. anoplus* suggests that it grew more slowly than *Procolophon* or *Teratophon*, whose bone tissues exhibit more highly vascularized parallel-fibered bone. However, the juvenile status of the *Sauropareion* specimen NMQR 3602 complicates an assessment of the overall growth patterns of this taxon as a later growth spurt cannot be ruled out (as seen in *Procolophon*). It is possible that the slow growth observed in *Sauropareion* was affected by its small body size because within a given clade, smaller animals grow more slowly than their larger relatives (Case, 1978; Padian et al., 2004). However, as fully adult individuals of *Sauropareion* have yet to be recovered, the maximum size of this taxon is currently unknown. Thus, more material is required before we can confirm that the

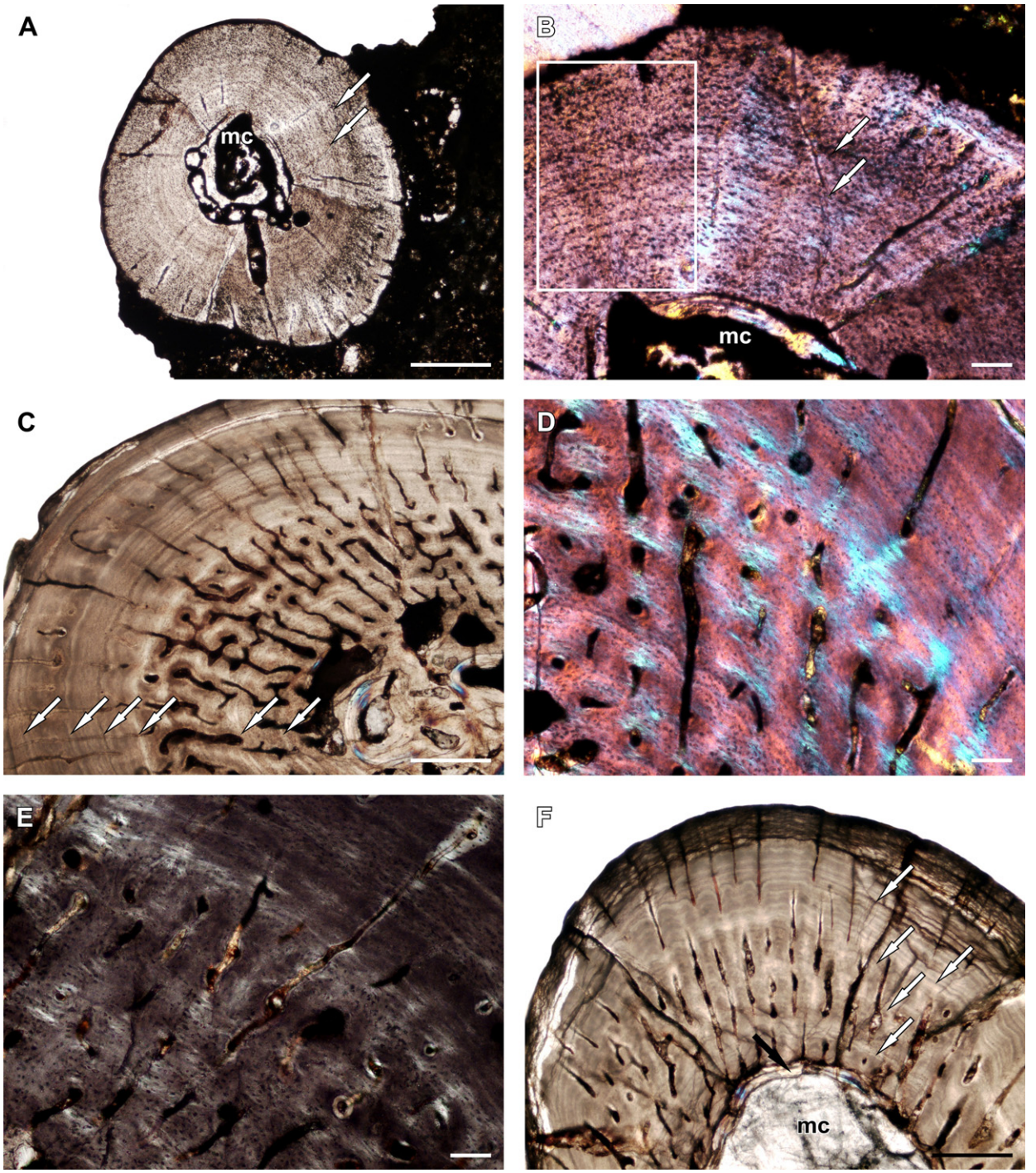

Fig. 6. Bone histology of *Teratophon spinigenis* and specimen SAM-PK-7711. **A**. Radius of SAM-PK-K10183 showing a poorly vascularized thick cortex with mostly radiating simple canals. Arrows indicate a change in bone tissue deposition rate. **B**. Radius of SAM-PK-K10183 in polarized light with Lambda compensator showing parallel-fibered bone and abundant osteocyte lacunae. Numerous Sharpey's fibers are also visible (box). Arrows indicate a change in bone tissue deposition rate. **C**. Humerus of SAM-PK-7711a taken slightly below the midshaft (hence the presence of bony trabeculae within the medullary cavity) showing highly vascularized inner bone tissue with a sub-reticular vascular arrangement and a poorly vascularized outer bone tissue with radiating simple vascular canals. Arrows indicate annuli. **D**. High magnification of humerus SAM-PK-7711a in polarized light with Lambda compensator taken at the midshaft showing highly vascularized parallel-fibered bone in the inner cortex. **E**. High magnification of humerus SAM-PK-7711a in polarized light taken at the midshaft showing parallel-fibered bone. **F**. Tibia of SAM-PK-7711b showing a radiating network of vascular canals and a prominence of annuli in the outer tissue. White arrows indicate annuli and black arrow indicates endosteal bone lining the medullary cavity. Abbreviations: mc: medullary cavity. Scale bars: (**A**, **C**, **F**) 500 μm; (**B**, **D**, **E**) 100 μm.

slow growth observed in *Sauropareion* is related to small body size.

The bone tissues of *P. trigoniceps* revealed initial slow growth early in ontogeny, indicated by the presence of sparse simple vascular canals. However, the growth rate increased in the sub-adults where an increase in vascularization was observed. All the elements studied are characterized by uninterrupted parallel-fibered bone. The bone tissue becomes more organized and vascularization decreases towards the subperiosteal surface in the ontogenetically older elements. However, annuli and LAG are absent from all individuals studied. Annuli and LAG, or growth rings, reflect endogenous biological rhythms that are reinforced by external factors (Castanet and Baez, 1991). They correspond to temporary cessations in growth (Francillon et al., 1990) and experiments on extant animals have shown them to be seasonal (Hutton, 1986). Thus, the absence of growth rings in *Procolophon* suggests that this taxon either reached adult size within one year or its growth rate was not affected by seasonal variation. The largest known skull of *Procolophon* is 78 mm in length and corresponds to a snout-vent length of 500 mm (Cisneros, personal communication, 2011). Small extant squamates such as agamids, chamaeleonids and gymnophthalmids (maximum snout-vent length 100 mm) generally reach sexual maturity within one year (Castanet, 1994; Dunham et al., 1988; James, 1991), whereas larger squamates such as *Varanus niloticus* (snout-vent length 1 m) usually reach sexual maturity after two years (Enge et al., 2004). The maximum known length of *Procolophon* falls between these ranges and although it may not reflect the maximum possible size of the genus, it can be considered an adult (based on morphology, Cisneros, personal communication, 2011). The bone tissues of *Procolophon* are notably more vascularized compared to those of extant squamates, indicating relatively higher growth rates (Amprino, 1947; de Margerie et al., 2002). Thus, although maximum size was probably not achieved within one year, it is possible that sexual maturity was achieved within this time frame. Sexual maturity has been shown to be associated with a dramatic change to a slowly forming bone tissue in extant taxa (e.g., amphibians and reptiles; Castanet and Baez, 1991; Castanet and Smirina, 1990; walrus *Odobenus rosmarus*, Klevezal, 1996) and possibly extinct taxa as well (non-avian dinosaurs, Reid, 1996, Sander, 2000; non-mammaliaform cynodont therapsids, Botha and Chinsamy, 2005; Botha-Brink and Angielczyk, 2010). The clear increased organization of the osteocyte lacunae into parallel rows accompanied by a dramatic decrease in vascularization in the outer cortex of humerus NMQR 3622a (approximately 77% of the maximum known size) suggests that sexual maturity had been reached because growth had decreased dramatically. Thus, if *Procolophon* exhibited growth rings at all, it would have been particularly late in ontogeny (and after the onset of sexual maturity).

The bone tissues of the Middle Triassic procolophonid *Teratophodon spinigenis* in this study differ from those of the Early Triassic. Although the radius of SAM-PK-K10183 revealed poorly vascularized parallel-fibered bone, the tibia and humerus of SAM-PK-7711 revealed inner cortices of highly vascularized (9% average inner cortical porosity) parallel-fibered bone tissue with radially-oriented vascular canals in the tibia and a reticular vascular arrangement in the humerus. Annuli were observed traversing the inner and mid-cortex, indicating that growth was intermittent. The bone tissue becomes poorly vascularized and multiple, closely spaced annuli appear towards the subperiosteal surface in both elements, suggesting that sexual maturity had been reached in this individual. The presence of annuli in the inner cortex prior to sexual maturity however, suggests that the growth of *Teratophon* was intermittent, even during early ontogeny. The presence of at least three annuli in SAM-PK-7711 for example, indicates that it took at least three years for this individual to reach sexual maturity. This pattern differs from that seen in *Procolophon* where growth rings are absent throughout ontogeny (even after sexual maturity had been reached).

The two larger procolophonid taxa (*Procolophon* and *Teratophon*) exhibit tissues that are fairly distinct from those of other reptiles. The bone tissues of *Sauropareion* are comparable with similar-sized extant squamates as well as the Permian diapsids *Youngina* and *Captorhinus* (personal observation, 2010). These animals contain poorly vascularized or avascular simple lamellar or parallel-fibered bone (Enlow and Brown, 1957; de Ricqlès, 1976; Laurin et al., 2011). However, it must be noted that all known specimens of *Sauropareion* are considered to be juveniles, and future recovery of more mature individuals will provide additional information on the overall growth patterns of this taxon. In contrast, the bone tissues of *Procolophon* and *Teratophon* differ from those of extant reptiles, in that the inner and mid-cortices of some elements are notably more vascularized (up to 10% cortical porosity) than even large *Varanus* species and crocodilians where juvenile cortical porosity only reaches 4.6% (1.6–1.9% in adults) (Chinsamy, 1993; de Buffrénil et al.,

Fig. 6. Histologie osseuse de *Teratophon spinigenis* et spécimen SAM-PK-7711. **A**. Radius de SAM-PK-K 10183 montrant un épais cortex faiblement vascularisé avec de simples canaux dont la plupart sont rayonnants. Les flèches indiquent un changement dans la vitesse de dépôt du tissu osseux. **B**. Radius de SAM-PK-K 10183 en lumière polarisée avec compensateur Lambda montrant un os à fibres parallèles et d'abondantes lacunes d'ostéocyte. De nombreuses fibres de Sharpey sont aussi visibles (rectangle blanc). Les flèches indiquent un changement dans la vitesse de dépôt du tissu osseux. **C**. Humérus de SAM-PK-7711a pris légèrement au-dessous de la mi-hauteur de l'axe (d'où la présence de travées osseuses au sein de la cavité médullaire) montrant un tissu osseux très vascularisé, avec un arrangement vasculaire sub-réticulé et un tissu osseux externe faiblement vascularisé, à simples canaux vasculaires rayonnants. Les flèches indiquent des anneaux. **D**. Fort grossissement d'humérus SAM-PK-7711a en lumière polarisée avec compensateur lambda pris à mi-hauteur de l'axe, montrant un os à fibres parallèles très bien vascularisés dans le cortex interne. **E**. Fort grossissement de l'humérus SAM-PK-K 77 11a en lumière polarisée, pris à mi-hauteur de l'axe montrant un os à fibres parallèles. **F**. Tibia de SAM-PK 7711b montrant un réseau rayonnant de canaux vasculaires et une proéminence d'anneaux dans le tissu externe. Les flèches blanches indiquent les anneaux et la flèche noire indique un os endostéen soulignant la cavité médullaire. Abréviations : mc : cavité médullaire. Barres d'échelle (**A**, **C**, **F**) 500 μm ; (**B**, **D**, **E**) 100 μm.

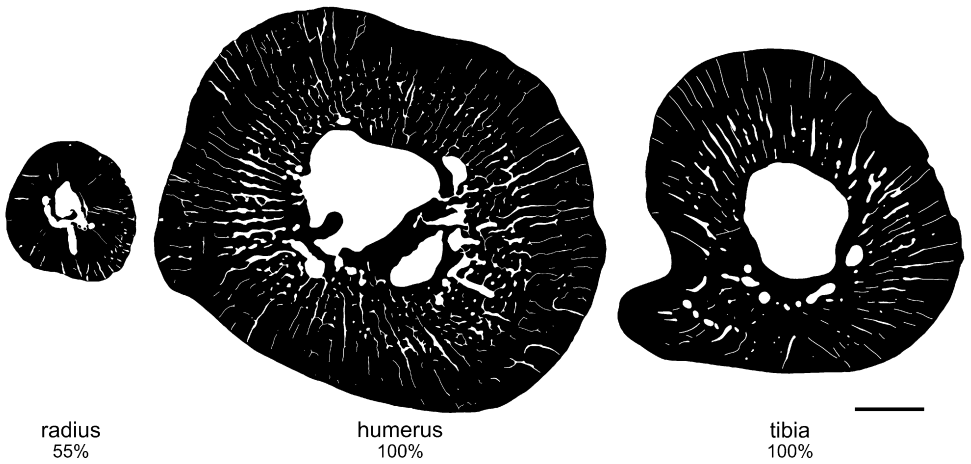

Fig. 7. Diaphyseal cross-sections of *Teratophon spinigenis* limb bones from the radius of SAM-PK-10183, and the humerus and tibia of SAM-PK-7711 (tentative assignment). Note the high vascularization in the inner cortices of the humerus and tibia and radiating vascular canals in the outer cortices. Percentages indicate percentage maximum size. Scale bar 1 mm.
Fig. 7. Coupes diaphysaires d'os de membre de *Teratophon spinigenis*, provenant de radius de SAM-PK-10183, d'humérus et de tibia de SAM-PK-7711 (identification incertaine). À noter la vascularisation importante des cortex internes d'humérus et de tibia et les canaux vasculaires rayonnants dans les cortex externes. Barre d'échelle 1 mm.

2008). The reticular vascular organization observed in the *Procolophon* femora and *Teratophon* humerus is also highly unusual in reptiles and is usually only found in extinct archosaurs that exhibit fibro-lamellar bone (some basal archosauromorphs and non-avian dinosaurs, Botha-Brink and Smith, 2011; de Ricqlès et al., 2008). Living crocodilians tend to exhibit poorly vascularized parallel-fibered or lamellar-zonal bone and the vascular orientation is predominantly longitudinal (Lee, 2004) even in juveniles less than one year old that exhibit fibro-lamellar bone (Horner et al., 2001). Few parareptiles have been subjected to bone histological analysis and thus, it is difficult to compare these procolophonids with other members of the group. De Ricqlès (1976) examined the limb bones of adult *Pareiasaurus* and more recently Scheyer and Sander (2009) studied the osteoderms of three pareiasaur species, namely *Pareiasaurus*, *Bradysaurus* and *Anthodon*. Both studies found poorly vascularized slowly forming lamellar-zonal bone tissues in these taxa. The vascular organization in the bone tissues of juvenile non-procolophonid parareptiles is not currently known, but hopefully, future research on these animals will confirm whether *Procolophon* and *Teratophon* can be distinguished from other medium to large Permian parareptiles (cf. Canoville and Chinsamy, 2011). It is possible that other small parareptiles (e.g. *Australothyris*, Millerettidae, other procolophonoids), most of which are similar in size to known individuals of *Sauropareion* (maximum known skull length 40 mm), exhibit relatively poorly vascularized parallel-fibered bone tissues, similar to this taxon. Simple poorly vascularized tissues are seen in numerous small extant animals such as lizards, moles, bats and the rhynchocephalian *Sphenodon* (Cubo et al., 2005; Enlow and Brown, 1957, 1958; Laurin et al., 2011). However, it should also be noted that recent studies have found vascular density to be more closely correlated with phylogeny or growth rate rather than body size (Cubo et al., 2005; de Buffrénil et al., 2008).

4.2. Triassic procolophonid palaeoecology

Sauropareion does not have any distinct postcranial adaptations for limb-based digging such as a short humerus, which is shorter in length than the femur, an elongated acromion process on the scapula or an elongated olecranon process on the ulna (Hildebrand, 1985; Kley and Kearney, 2007). However, it does have several features, such as a prominent spade-shaped skull, relatively large unguals (40% longer than the penultimate phalanges) and short, robust non-terminal phalanges (that would rigidify the manus and pes against forces incurred during digging), which suggests that it may have used head-assisted, fore- and hind limb scratch-digging (MacDougall et al., in press). Furthermore, the proportion of the epicondylar width to the total length of the humerus is 0.48, which falls within the range for scratch-diggers (which range from 0.2 to 0.7) and is well above that of most non-fossorial animals (≤ 0.2) (Hildebrand, 1985). The humerus of the juvenile *Sauropareion* individual examined in this study has a moderately thick cortex ($k = 0.56$), indicating that the propodials of this genus were relatively robust (compared to many extant iquanid lizards, which have thinner humeral cortices, average $k = 0.68$; Laurin et al., 2011). Thus, we support the proposal that *Sauropareion* may have been a scratch-digger that used its spade-shaped skull to aid in moving and packing soil, as has been observed in extant mammals such as moles and mole-rats (Hildebrand, 1985; Wake, 1993).

Numerous studies have suggested that *Procolophon* was a burrower (e.g., Botha-Brink and Modesto, 2007; deBraga, 2003; Groenewald, 1991; Miller et al., 2001) and there are several morphological characteristics of the skull and skeleton to support such a lifestyle. For example, deBraga (2003) noted that the short, triangular-shaped skull, concave, spade-shaped dorsal skull surface, distinct overbite (possibly to reduce ingestion of dirt), robust limb bones and large, broad unguals would have been useful for digging. *Procolophon* also has relatively short epipodials and

a broad rib cage, features that are frequently observed in digging animals (Hildebrand, 1974), and the epicondylar width to humeral length ratio is 0.53, well within the range of scratch-diggers (Hildebrand, 1985). Furthermore, it is common for numerous *Procolophon* fossils to be collected in close association (e.g. "*Procolophon* hill" locality of Kitching, 1977) and some specimens have even been recovered from interpreted burrow casts (Groenewald, 1991). The humerus of *Procolophon* has a relatively thick cortex (average $k = 0.49$) and is thicker than many iguanid lizards (Laurin et al., 2011) including the large burrowing desert monitor *Varanus griseus* ($k = 0.5072$), which averages 1 m in snout-vent length. Thick cortices, which aid in countering large compressive stresses, have also been found in several extant digging mammals such as insectivores and rodents (Biknevicius, 1993; Bou et al., 1990). Thus, the combined observations in taphonomic style, functional morphology and bone microstructure (moderately thick cortex and prominent Sharpey's fibers indicating the need for strong muscle insertions, which would be necessary for a demanding activity such as digging) supports previous suggestions that *Procolophon* was capable of burrowing and may have excavated burrows using both the head and forelimbs.

Several burrow casts have also been found in association with *Teratophon* specimens in the *Cynognathus* Assemblage Zone (personal observation, 2003). *Teratophon* has a particularly thick cortex in all the elements studied (average $k = 0.3$). The limb bones are thicker than the burrowing rodent *Ctenomys* ($k = 0.5$, Biknevicius, 1993), as well as many extant iguanid, anguid and teiid lizards, and is most similar to the burrowing *V. griseus* ($k = 0.3$) and marine iguana, *Amblyrhynchus cristatus* ($k = 0.38$), both of which have notably thick cortices (Laurin et al., 2011). The epicondylar width to humeral length ratio is 0.48, which is comparable to the pangolin (Hildebrand, 1985), which is fossorial. The morphology of *Teratophon*, which includes large, robust limbs and unguals, short robust non-terminal phalanges, and thickened cortices suggest that it was capable of digging the burrows found in association with it, and may also have been semi-fossorial (i.e. an animal that has some skeletal adaptations for digging, but not extreme morphological specializations; Dunn and Rasmussen, 2007), similar to *Sauropareion* and *Procolophon*. Moreover, individuals of *Sauropareion*, *Procolophon* and *Teratophon* tend to be found in groups (Kitching, 1977; personal observation, 2011). For example, three of the five known *Sauropareion* specimens were found within a few meters of one another. These accumulations are emphasized in *Teratophon* and particularly in *Procolophon*, which are often found grouped together in high abundance to form monospecific aggregations (Kitching, 1977). Burrowing has been suggested for other procolophonids as well, such as *Hypsognathus fenneri* (Sues et al., 2000), *Koiloskiosaurus coburgensis* (Botha-Brink and Modesto, 2007) and *Leptopleuron lacertinum* (Säilä, 2010). Most living reptiles are capable diggers, even those lacking skeletal modifications for digging (deBraga, 2003; Voorhies, 1975). Thus the overall trend of increased robustness in procolophonids together with the various morphological and histological modifications in these taxa suggests that a fossorial lifestyle was a general behavioral trait in the Procolophonidae (deBraga, 2003).

4.3. Triassic procolophonids and the end-Permian extinction event

Although it has yet to be confirmed in *Sauropareion* (due to the lack of confirmed adult material), the absence of growth rings in *Procolophon* is noteworthy. Extant reptiles exhibit periodic decreases or cessations in growth during the unfavorable season (Peabody, 1961) and as the climate of the Early Triassic South African Karoo Basin was strongly seasonal (Smith and Botha, 2005), it is expected that *Procolophon* would have exhibited such growth rings. However, they are absent. In contrast, *Teratophon* grew intermittently, even during early ontogeny, similar to extant and most extinct reptiles. This suggests a difference in life history between Early and Middle Triassic South African procolophonids. The relatively high vascularization during early growth in *Procolophon* and Middle Triassic procolophonids, which is higher than that of extant reptiles, also suggests relatively rapid early growth as vascularization is closely related to growth rate (de Margerie et al., 2002), albeit in a parallel-fibered matrix, which represents slower growth rates than fibro-lamellar bone.

Burrowing has been shown to lower the extinction risk in extant mammals by providing a temporary refuge against predators and unexpected environmental changes (Liow et al., 2009). This behavior has also been proposed as a survival strategy for numerous Early Triassic vertebrates (e.g. the dicynodont *Lystrosaurus*, non-mammaliaform cynodonts, therocephalians) as a means of escaping the unpredictable environmental conditions of that time (Bordy et al., 2011; Botha and Smith, 2006; Smith and Botha-Brink, 2009). The Early Triassic is characterized by extreme temperatures, aridity and unpredictable rainfall (Botha and Smith, 2006; Roopnarine et al., 2007; Smith and Ward, 2001), but procolophonoids appear to have been relatively unaffected by the end-Permian extinction (Botha et al., 2007; Modesto et al., 2001, 2003). They are the only parareptile group that crossed the Permo-Triassic boundary and then radiated extensively during the Early Triassic. It is possible that early relatively rapid growth (compared to other non-archosaurian reptiles), constant growth rate (i.e. little susceptibility to seasonal fluctuations) and/or fossorial behavior were advantageous in the post-extinction environment, allowing *Procolophon* to become the most widespread and abundant parareptile of the Early Triassic.

Acknowledgments

Thank you to the National Museum, Bloemfontein and Iziko South African Museums for the loan of material. We thank J. Nyaphuli, J. Mohoi and N. Nthaopa of the National Museum, Bloemfontein for the mechanical preparation of the study material. Michel Laurin, Kevin Padian and two anonymous reviewers are kindly acknowledged for their helpful comments on an earlier draft of this manuscript. This project was funded by a joint research grant from the

National Research Foundation of South Africa to J.B.B. and R.M.H.S. (UID65241).

References

Amprino, R., 1947. La structure du tissu osseux envisage comme expression de differences dans la vitesse de l'accroissement. Arch. Biol. 58, 315–330.

Biknevicius, A.R., 1993. Biomechanical scaling of limb bones and differential limb use in caviomorph rodents. J. Mammal. 74, 95–107.

Bordy, E.M., Sztanó, O., Rubidge, B.S., Bumby, A., 2011. Early Triassic vertebrate burrows from the Katberg Formation of the south-western Karoo Basin, South Africa. Lethaia 44, 33–45.

Botha, J., 2003. Biological aspects of the Permian dicynodont *Oudenodon* (Therapsida, Dicynodontia), deduced from bone histology and cross-sectional geometry. Palaeontol. Afr. 39, 37–44.

Botha, J., Chinsamy, A., 2005. Growth patterns of *Thrinaxodon*, a non-mammalian cynodont from the Early Triassic of South Africa. Palaeontology 48, 85–394.

Botha, J., Smith, R., 2006. Rapid vertebrate recuperation in the Karoo Basin of South Africa following the end-Permian extinction. J. Afr. Earth Sci. 45, 502–514.

Botha-Brink, J., Modesto, S.P., 2007. A mixed-age classed "pelycosaur" aggregation from South Africa: earliest evidence of parental care in amniotes? Proc. R. Soc. B 274, 2829–2834.

Botha-Brink, J., Angielczyk, K.D., 2010. Do extraordinarily high growth rates in Permo-Triassic dicynodonts (Therapsida, Anomodontia) explain their success before and after the end-Permian extinction? Zool. J. Linn. Soc. 160, 341–365.

Botha-Brink, J., Smith, R.M.H., 2011. Osteohistology of the Triassic archosauromorphs *Prolacerta*, *Proterosuchus*, *Euparkeria* and *Erythrosuchus* from the Karoo Basin of South Africa. J. Vert. Paleontol. 31, 1238–1254.

Botha, J., Modesto, S., Smith, R., 2007. Extended procolophonoid reptile survivorship after the end-Permian extinction. S. Afr. J. Sci. 103, 54–56.

Bou, J., Castiella, M.J., Ocana, J., Casinos, A., 1990. Multivariate analysis and locomotor morphology in insectivores and rodents. Zool. Anz. 225, 287–294.

Canoville, A., Laurin, M., 2010. Evolution of humeral microanatomy and lifestyle in amniotes, and some comments on palaeobiological inferences. Biol. J. Linn. Soc. 100, 384–406.

Canoville, A., Chinsamy, A., 2011. Palaeobiology of pareiasaurs (Parareptilia, Pareiasauridae) inferred from long bone histology and microanatomy. 1st Internat. Symp. Paleohistol., Sabadell, Spain, 51.

Case, T.J., 1978. Speculations on the growth rate and reproduction of some dinosaurs. Paleobiology 4, 320–328.

Castanet, J., 1994. Age estimation and longevity in reptiles. Gerontology 40, 174–192.

Castanet, J., Baez, M., 1991. Adaptation and evolution in *Gallotia* lizards from the Canary Islands: age, growth, maturity and longevity. Amphibia-Reptilia 12, 81–102.

Castanet, J., Smirina, E., 1990. Introduction to the skeletochronological method in amphibians and reptiles. Ann. Sci. Nat. Zool. 11, 191–196.

Chinsamy, A., 1993. Image analysis and the physiological implications of the vascularization of femora in archosaurs. Mod. Geol. 19, 101–108.

Chinsamy, A., Raath, M.A., 1992. Preparation of fossil bone for histological examination. Palaeontol. Afr. 29, 3–44.

Cisneros, J.C., 2008. Taxonomic status of the reptile genus *Procolophon* from the Gondwanan Triassic. Palaeontol. Afr. 43, 7–17.

Cubo, J., Pontin, F., Laurin, M., de Margerie, E., Castanet, J., 2005. Phylogenetic signal in bone microstructure of sauropsids. Syst. Biol. 54, 562–574.

Currey, J.D., Alexander, R.M., 1985. The thickness of the walls of tubular bones. J. Zool. 206, 453–468.

deBraga, M., 2003. The postcranial skeleton, phylogenetic position, and probable lifestyle of the Early Triassic reptile *Procolophon trigoniceps*. Can. J. Earth Sci. 40, 527–556.

de Buffrénil, V., Houssaye, A., Böhme, W., 2008. Bone vascular supply in monitor lizards (Squamata: Varanidae): influence of size, growth, and phylogeny. J. Morph. 269, 533–543.

de Buffrénil, V., de Ricqlès, A., Ray, C.E., Domning, D.P., 1990. Bone histology of the ribs of the archaeocetes (Mammalia: Cetacea). J. Vert. Paleontol. 10, 455–466.

de Margerie, E., Cubo, J., Castanet, J., 2002. Bone typology and growth rate: testing and quantifying "Amprino's rule" in the mallard (*Anas platyrhynchos*). C. R. Biologies 325, 221–230.

de Ricqlès, A., 1976. On bone histology of fossil and living reptiles, with comments on its functional and evolutionary significance. In: Bellairs, d'A., Cox, A., C.B. (Eds.), Morphology and Biology of Reptiles. Academic Press, London, pp. 123–150.

de Ricqlès, A., Padian, K., Knoll, F., Horner, J.R., 2008. On the origin of high growth rates in archosaurs and their ancient relatives: complementary histological studies on Triassic archosauriforms and the problems of a "phylogenetic signal" in bone histology. Ann. Paleontol. 94, 57–76.

Dunham, A.E., Miles, D.B., Reznick, D.N., 1988. Life history patterns in squamate reptiles. In: Gans, C., Huey, R.B. (Eds.), Biology of the Reptilia. Alan R. Liss, New York, pp. 441–522.

Dunn, R.H., Rasmussen, D.T., 2007. Skeletal morphology and locomotor behavior of *Pseudotomus eugenei* (Rodentia, Paramyinae) from the Uinta Formation, Utah. J. Vert. Paleont. 27, 987–1006.

Enge, K.M., Krysko, K.L., Hankins, K.R., Campbell, T.S., King, F.W., 2004. Status of the Nile Monitor (*Varanus niloticus*) in southwestern Florida. Southeas. Nat. 3, 571–582.

Enlow, D.H., Brown, S.O., 1957. A comparative histological study of fossil and recent bone tissues. Part II. Tex. J. Sci. 9, 186–214.

Enlow, D.H., Brown, S.O., 1958. A comparative histological study of fossil and recent bone tissues. Part III. Tex. J. Sci. 9, 187–230.

Francillon-Vieillot, H., de Buffrénil, V., Castanet, J., Geraudie, J., Meunier, F.J., Sire, J.Y., Zylberberg, L., de Ricqlès, A., 1990. Microstructure and mineralization of vertebrate skeletal tissues. In: Carter, J.G. (Ed.), Skeletal Biomineralization: Patterns, Processes and Evolutionary Trends. Van Nestrand Reinhold, New York, pp. 471–548.

Germain, D., Laurin, M., 2005. Microanatomy of the radius and lifestyle in amniotes (Vertebrata, Tetrapoda). Zool. Script. 34, 335–350.

Girondot, M., Laurin, M., 2003. Bone Profiler: a tool to quantify, model, and statistically compare bone-section compactness profiles. J. Vert. Paleontol. 23, 458–461.

Gow, C.E., 2000. A new procolophonid (Parareptilia) from the *Lystrosaurus* Assemblage Zone, Beaufort Group, South Africa. Palaeontology 36, 21–23.

Groenewald, G.H., 1991. Burrow casts from the *Lystrosaurus-Procolophon* Assemblage-zone, Karoo Sequence, South Africa. Koedoe 34, 13–22.

Hildebrand, M., 1974. Analysis of vertebrate structure. John Wiley & Sons, New York, 709 p.

Hildebrand, M., 1985. Digging of quadrupeds. In: Hildebrand, M., Bramble, D.M., Liem, K.F., Wake, D.B. (Eds.), Functional Vertebrate Morphology. Harvard University Press, Cambridge, pp. 89–109.

Horner, J.R., de Ricqlès, A., Padian, K., 1999. Variation in dinosaur skeletochronology indicators: implications for age assessment and physiology. Paleobiology 25, 295–304.

Horner, J.R., de Ricqlès, A., Padian, K., 2001. Comparative osteohistology of some embryonic and perinatal archosaurs: phylogenetic and behavioral implications for dinosaurs. Paleobiology 27, 39–58.

Hua, S., de Buffrénil, V., 1996. Bone histology as a clue in the interpretation of functional adaptations in the Thalattosuchia (Reptilia, Crocodylia). J. Vert. Paleontol. 16, 703–717.

Hutton, J.M., 1986. Age determination of living Nile crocodiles from the cortical stratification of bone. Copeia 2, 332–341.

James, C.D., 1991. Growth rates and ages at maturity of sympatric scincid lizards (*Ctenotus*) in Central Australia. J. Herp. 25, 284–295.

Kitching, J.W., 1977. The distribution of the Karroo vertebrate fauna. Johannesburg, Bernard Price Institute for Palaeontological Research, University of the Witwatersrand, Memoir 1, 1–131.

Klevezal, G.A., 1996. Recording structures of mammals. Determination of age and reconstruction of life history. A. A. Balkema, Rotterdam, 274 p.

Kley, N.J., Kearney, M., 2007. Adaptations for digging and burrowing. In: Hall, B.K. (Ed.), Fins into Limbs: evolution, Development, and Transformation. University of Chicago Press, Chicago, pp. 284–309.

Kriloff, A., Germain, D., Canoville, A., Vincent, P., Sache, M., Laurin, M., 2008. Evolution of bone microanatomy of the tetrapod tibia and its use in palaeobiological inference. J. Evol. Biol. 21, 807–826.

Lagaria, A., Youlatos, D., 2006. Anatomical correlates to scratch digging in the forelimb of European ground squirrels (*Spermophilus citellus*). J. Mammal. 87, 563–570.

Laurin, M., Girondot, M., Loth, M.-M., 2004. The evolution of long bone microanatomy and lifestyle in lissamphibians. Paleobiology 30, 589–613.

Laurin, M., Canoville, A., Germain, D., 2011. Bone microanatomy and lifestyle: a descriptive approach. C. R. Palevol 10, 381–402.

Lee, A.H., 2004. Histological organisation and its relationship to function in the femur of *Alligator mississippiensis*. J. Anat. 204, 197–207.

Liow, L.H., Fortelius, M., Lintulaakso, K., Mannila, H., Stenseth, N.C., 2009. Lower extinction risk in sleep-or-hide mammals. Am. Nat. 173, 264–272.

MacDougall, M.J., Modesto, S.P., Botha-Brink, J., in press. The postcranial skeleton of the Early Triassic parareptile *Sauropareion anoplus*, with a discussion of possible life history. Acta Palaeontol. Pol.

Miller, M.F., Hasiotis, S.T., Babcock, L.E., Isbell, J.L., Collinson, J.W., 2001. Tetrapod and large burrows of unknown origin in Triassic high paleolatitude floodplain deposits, Antarctica. Palaios 16, 218–232.

Modesto, S.P., Damiani, R., 2003. Taxonomic status of *Thelegnathus browni* Broom, a procolophonid reptile from the South African Triassic. Ann. Carnegie Mus. 72, 53–64.

Modesto, S.P., Damiani, R., 2007. The procolophonoid reptile *Sauropareion anoplus* from the lowermost Triassic of South Africa. J. Vert. Paleontol. 27, 337–349.

Modesto, S., Sues, H.-D., Damiani, R., 2001. A new Triassic procolophonoid reptile and its implications for procolophonoid survivorship during the Permo-Triassic extinction event. Proc. R. Soc. Lond. B 268, 2047–2052.

Modesto, S., Damiani, R., Neveling, J., Yates, A.M., 2003. A new Triassic owenettid parareptile and the Mother of Mass Extinctions. J. Vert. Paleontol. 23, 715–719.

Modesto, S.P., Scott, D.M., Botha-Brink, J., Reisz, R.R., 2010. A new and unusual procolophonid parareptile from the Lower Triassic Katberg Formation of South Africa. J. Vert. Paleontol. 30, 715–723.

Mundil, R., Ludwig, K.R., Metcalf, I., Renne, P.R., 2004. Age and timing of the Permian mass extinctions: U/Pb dating of closed-system zircons. Science 305, 1760–1763.

Padian, K., Horner, J.R., de Ricqlès, A., 2004. Growth in small dinosaurs and pterosaurs: the evolution of archosaurian growth strategies. J. Vert. Paleontol. 24, 555–571.

Peabody, F.E., 1961. Annual growth zones in living and fossil vertebrates. J. Morph. 108, 11–62.

Reid, R.E.H., 1996. Bone histology of the Cleveland-Lloyd dinosaurs and of dinosaurs in general, part I: introduction: introduction to bone tissues. Brigham Young University Geology Studies 41, 25–71.

Roopnarine, P.D., Angielczyk, K.D., Wang, S.C., Hertog, R., 2007. Food web models explain instability of Early Triassic terrestrial communities. Proc. R. Soc. B 274, 2077–2086.

Ruta, M., Cisneros, J.C., Liebrecht, T., Tsuji, L.A., Müller, J., 2011. Amniotes through major biological crises: faunal turnover among parareptiles and the end-Permian mass extinction. Palaeontology 54, 1475–4983.

Säilä, L.K., 2010. Osteology of *Leptopleuron lacertinum* Owen, a procolophonoid parareptile from the Upper Triassic of Scotland, with remarks on ontogeny, ecology and affinities. Earth Environ. Sci. Trans. R. Soc. Edinburgh 101, 1–25.

Sander, P.M., 2000. Longbone histology of the Tendaguru sauropods: implications for growth and biology. Paleobiology 26, 466–488.

Scheyer, T.M., Sander, P.M., 2009. Bone microstructures and mode of skeletogenesis in osteoderms of three pareiasaur taxa from the Permian of South Africa. J. Evol. Biol. 22, 1153–1162.

Smith, R., Botha, J., 2005. The recovery of terrestrial vertebrate diversity in the South African Karoo Basin after the End-Permian extinction. C. R. Palevol. 4, 555–568.

Smith, R.M.H., Botha-Brink, J., 2009. Burrowing as a survival strategy in the earliest Triassic Karoo Basin, South Africa. J. Vert. Paleont. SVP Program and Abstracts Book, 2009, 183A.

Smith, R.M.H., Ward, P.D., 2001. Pattern of vertebrate extinctions across an event bed at the Permian-Triassic boundary in the Karoo Basin of South Africa. Geology 29, 1147–1150.

Starck, J.M., Chinsamy, A., 2002. Bone microstructure and developmental plasticity in birds and other dinosaurs. J. Morph. 254, 232–246.

Sues, H.-D., Olsen, P.E., Scott, D.M., Spencer, P.S., 2000. Cranial osteology of *Hypsognathus fenneri*, a latest Triassic procolophonid reptile from the Newark Supergroup of eastern North America. J. Vert. Paleontol. 20, 275–284.

Tsuji, L.A., Müller, J., 2009. Assembling the history of the Parareptilia: phylogeny, diversification, and a new definition of the clade. Fossil Record 12, 71–81.

Voorhies, M.R., 1975. Vertebrate burrows. In: Frey, R.W. (Ed.), The Study of Trace Fossils. Springer, New York, pp. 325–350.

Wake, M.H., 1993. The skull as a locomotor organ. In: Hanken, J., Hall, B.K. (Eds.), The Skull. Volume 3, Functional and Evolutionary Mechanisms. University of Chicago Press, Chicago, pp. 197–240.

Wall, W.P., 1983. The correlation between limb-bone density and aquatic habits in recent mammals. J. Vert. Paleont. 57, 197–207.